Electronic Supplementary Material (ESI) for Environmental Science: Processes & Impacts.

SUPPLEMENTARY INFORMATION

Photolysis of the nonsteroidal anti-inflammatory drug sulindac: elucidation of kinetic behaviour and photodegradation pathways in water

Aura Ledezma-Espinoza[1*], Jonathan K. Challis[2], Floria Roa-Gutiérrez[1]; Andrés Sánchez-Kopper[1], Erick Castellón[3], Charles S. Wong[1,4]

[1] Centro de Investigación y de Servicios Químicos y Microbiológicos (CEQIATEC), School of Chemistry, Instituto Tecnológico de Costa Rica, Cartago 159-7050, Costa Rica.

[2]Toxicology Centre, University of Saskatchewan, Saskatoon, SK S7N 5B3, Canada.

[3] School of Chemistry, Materials Science and Engineering Research Center (CICIMA), Universidad de Costa Rica, San José 11501-2060, Costa Rica.

[4]Southern California Coastal Water Research Project Authority, Costa Mesa CA 92626 USA.

*Corresponding author: Tel: +506 2550 2733 ; E-mail: aledezma@itcr.ac.cr

MATERIALS AND METHODS

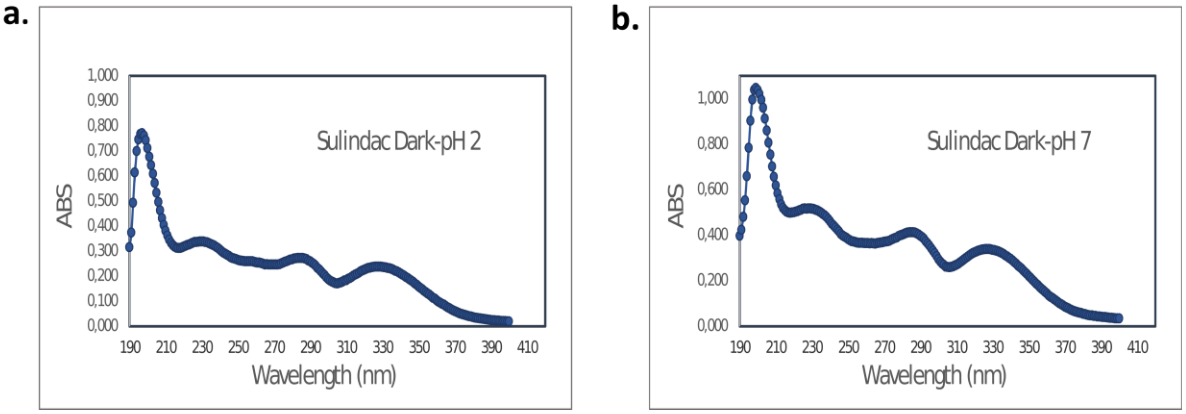

Figure S1. UV-VIS spectra of *Z*-sulindac solutions in water without UV irradiation at (a) pH2 and (b) pH7 conditions. UV/VIS-HPLC analysis were performed using the absorption-maximum wavelengths (λmax, nm) determined from these spectra.

Table S1: Gradient elution method for Qtof-MS Liquid Chromatography in sulindac analysis. Solvents were H_2O:0.05 % formic acid (A) and Methanol: 0.05 % formic acid (B).

Time (min)	Flow (mL/min)	% A	% B
0	0.3	95	5
1	0.3	95	5
2.5	0.3	50	50
4.0	0.3	50	50
6.5	0.3	5	95
7.5	0.3	5	95
11.5	0.3	95	5

RESULTS AND DISCUSSION

Direct photolysis experiments under laboratory conditions

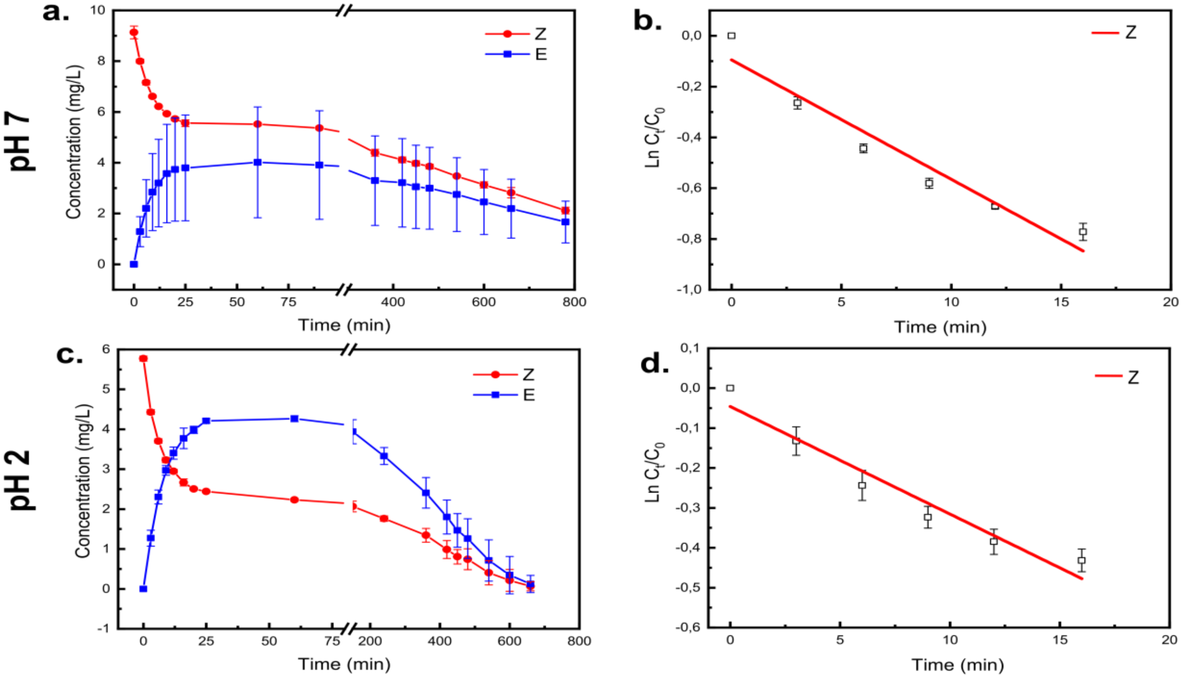

Figure S2. Time course profile for *Z* and *E* isomers concentrations during the photolysis of *Z*-sulindac solutions in water under UV-B irradiation with (a) pH7 and (c) pH2 conditions. Figures on the right side represent pseudo first-order kinetics for *Z*-sulindac at early stage of treatment with same irradiation under (b) pH7 and (d) pH2 conditions.

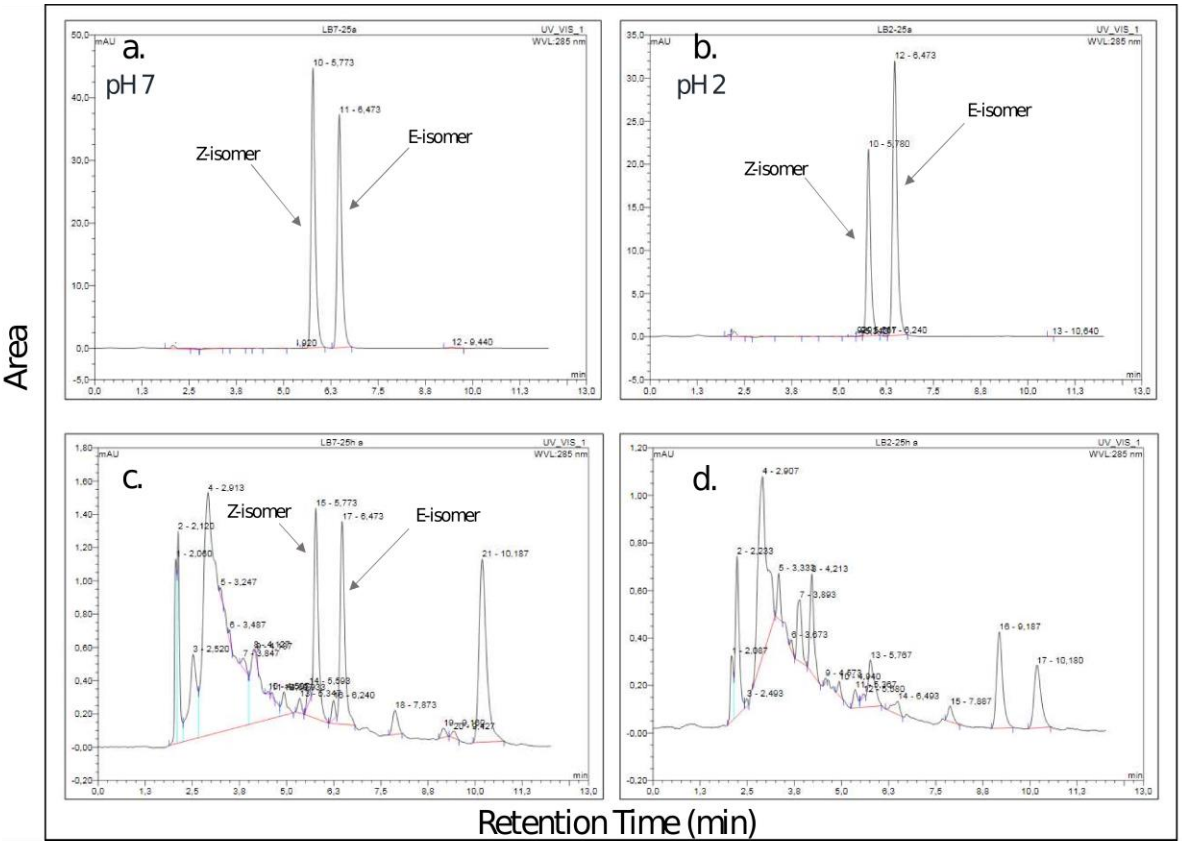

Figure S3. LC-UV/VIS trace for an isomeric photoproduct mixture of sulindac, generated with UV-B irradiation under conditions of (a) 25 min-pH 7, (b) 25 min-pH 2 and (c) 25 h-pH 7. Signals for isomers were no detected under (d) 25 h-pH 7 conditions ($\lambda_{detection}$ =285 nm).

Kinetic mechanism using the approach of consecutive reactions.

Model description

For simplicity, in the postulated mechanism (system equation 3), all the species are assumed to be in their neutral form, and P represents any degradation product. Stage 3b is the reversed isomerization of 3a. Reactions from 3a to 3d are unimolecular, and accordingly are considered as first order processes. Steps 3e and 3f involve bimolecular reactions of each isomer with any product P, generating additional products following second order reactions. Structural similarity between the *E* and *Z* isomers support the assumption that steps 3c and 3d have the same first order rate constant, k_2. The latter assumption additionally is used to estimate that steps 3e and 3f also take place with identical second-order specific rate constants, k_3.

Interpretation of model outputs are described below. Equation S4 provided the half-life of total sulindac concentration ($c_S = c_Z + c_E$) over time, depending on initial concentrations (eq. S5 and S6). The time variation of the total concentration of sulindac ($c_S = c_Z + c_E$) was fitted with the model equation S5 to calculate the specific rates k_2 and k_3. Further, fitted parameters were used to estimate $k_1$and k_{-1}.

Equation system S2. Calculation of molar absorptivity ratio sulindac isomers ($\boldsymbol{\varepsilon_Z/\varepsilon_E}$)

To calculate ($\boldsymbol{\varepsilon_Z/\varepsilon_E}$) ratio, absorbance *A* correspond to the wavelength of maximum absorption at the irradiation time (0 and 25 min), c_{Z0} is the sulindac concentration without irradiation (t=0), b is the pathlength, a is the error, and K is the photoequilibrium constant for the isomerization reaction. Measurements were made for three standard solutions with different initial concentrations of *Z*-sulindac (2, 7, and 10 mg/L) under each pH (2 and 7) and irradiation source (326 nm and 285 nm).

$$A = \varepsilon_Z\, bc_Z + \varepsilon_E bc_E + a \qquad (S2a)$$

$$\varepsilon_Z = \frac{A_0 - a}{b\, c_{Z0}} \qquad (S2b)$$

$$K = \frac{c_E}{c_Z} \qquad (S2c)$$

$$c_{Z0} = c_Z + c_E \qquad (S2d)$$

$$A = \frac{c_{Z0}\, K\, b\, \varepsilon_E}{K+1} + \frac{(A_0 - a)}{K+1} + a \qquad (S2e)$$

Differential equation model S4. Evaluation for the irradiation time dependence of the process according to the postulated mechanism (system equation 3):

$$\frac{dc_Z}{dt} = -k_1 c_Z + k_{-1} c_E - k_2 c_Z - k_3 c_Z c_P \qquad (S4a)$$

$$\frac{dc_E}{dt} = k_1 c_Z - k_{-1} c_E - k_2 c_E - k_3 c_E c_P \qquad (S4b)$$

$$\frac{dc_P}{dt} = k_2 c_Z + k_2 c_E + k_3 c_Z c_P + k_3 c_E c_P \qquad (S4c)$$

where c_J represents the concentration of J as function of time and initial conditions are considered as $c_Z(0) = z_0$, $c_E(0) = 0$ and $c_P(0) = 0$. It is to be highlighted, that the system of differential equations S4 cannot be analytically solved (i.e., the mathematical functions of time for the concentrations cannot be expressed in explicit forms). However, the variation with time regarding to the total concentration of sulindac ($c_S = c_Z + c_E$) could be solved as an explicit function:

$$c_S = c_Z + c_E = \frac{z_0(z_0 k_3 + k_2)}{k_2 e^{t(z_0 k_3 + k_2)} + z_0 k_3}. \qquad (S5)$$

According to equation S5, the half-life of total sulindac depends on its initial concentration as follows:

$$t_{1/2} = \frac{1}{z_0 k_3 + k_2} \ln\left(\frac{z_0 k_3 + 2k_2}{k_2}\right). \qquad (S6)$$

Following the above analysis, the time variation of the total concentration of sulindac $c_S = c_Z + c_E$ was fitted with the model equation S5 to calculate the specific rates k_2 and k_3 through the Levenberg-Marquardt algorithm for non-linear regression. The fitted parameters were used for the numerical solution of the system of differential equations S4. The estimation of $k_1$and k_{-1} was achieved with a numerical procedure of minimization of squared residuals written in the software

Maple for symbolic and numeric computation. The procedure was applied to fit the parametrized numeric solutions of the equation system S4, using the Runge-Kutta-Fehlberg method with fourth degree interpolant.

Validation of model

The model fitting was validated on criterion for goodness-of-fit and error analysis. Figure S4 illustrates the agreement between model and experimental findings. The standard deviation (SD) of the nonlinear regressions was considered to describe the maximum error for the model. According fitted model data for UV-A experiment at pH7, it can be stated that for a value of SD=0.129 mg/L, the maximum error in the modeled concentrations is predicted as 2SD=0.258 mg/L for 95% confidence. Therefore, the error of the regressions confirm the reliability of the proposed model to explain the experimental observations. Moreover, goodness-of-fit for each incubation system (Figure S4) showed that most of the modeled concentrations are similar to the experimental values, due all the points lining up close to the identity function (model=experimental), which indicates that the proposed kinetic model of consecutive reaction is valid and makes a reliable prediction of the sulindac degradation process induced by direct photolysis.

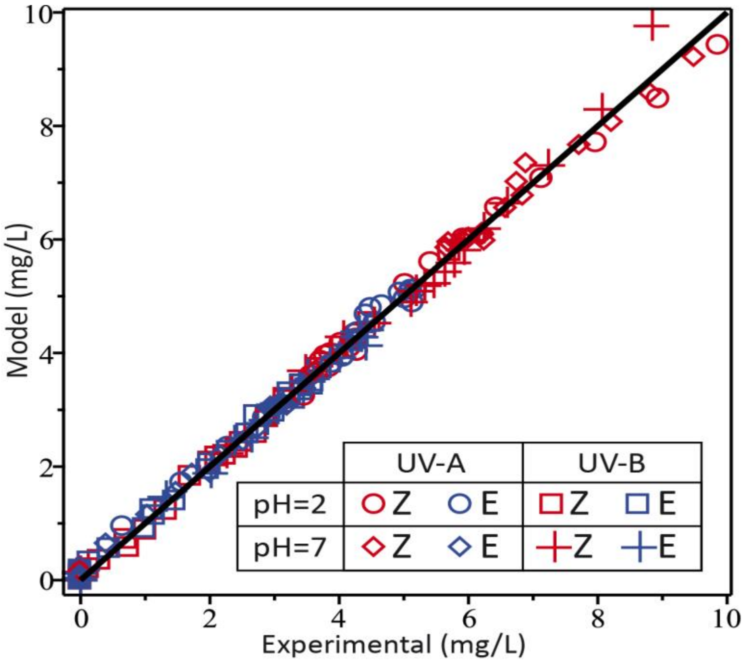

Figure S4. Modeled versus experimental concentrations of sulindac isomers. Modeled results from fitted differential equation system S4 following the proposed chemical mechanism of equation system 3. The black line represents the identity function (model=experimental).

Degradation byproducts and transformation pathway under experimental conditions.

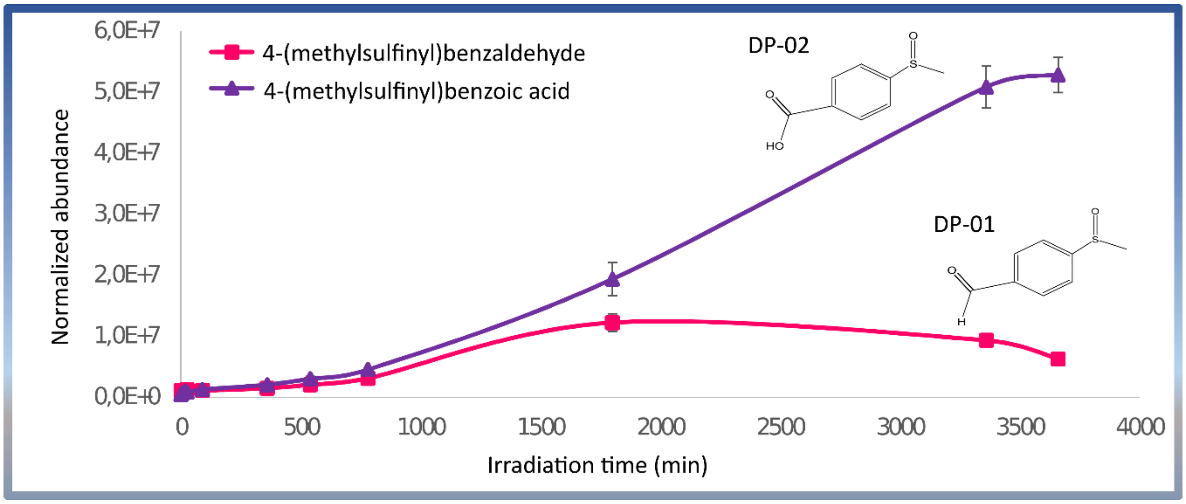

Figure S5. Monitoring of byproducts during sulindac photolysis by Qtof-MS compounds abundance profile under UV-A irradiation and pH 7 using Progenesis software. Data from replicates using average normalized abundance, standard deviations (SD) as errors, maximum fold Change>2 and Anova p-value≤0.05.

Table S2: Predicted aquatic toxicity of sulindac and photodegradation products by ECOSAR[a].

Compund	***Z*-sulindac** Parent compound	**DP-01** Aldehyde	**DP-02** Carboxylic acid
Structure	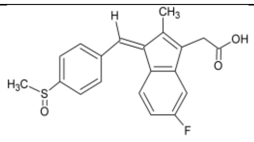	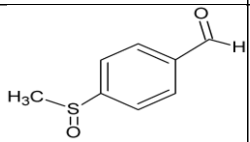	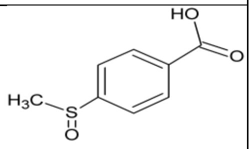
Log K_{OW}	3.4[b]	0.15[c]	0.31[c]
pKa	4.7	-	-
Estimated Solubility (mg/L)	3000	47000	28000
Predicted acute and chronic toxicity (mg/L)			
ECOSAR class	Neutral organics	Aldehydes (Mono)	Neutral organics
Green Algae EC50 (96 h)	33	41	9400
Daphnid LC50 (48 h)	18	86	24000
Fish LC50 (96 h)	26	79	50000[d]
Green Algae (ChV)	14	12	1700
Daphnid (ChV)	3.2	0.67	1500
Fish (ChV)	3.3	28	4000

[a]EPA (Version 2.0, accessed date: July 2021). [b]Measured. [c]Selected. [d]Chemical may not soluble enough to measure the predicted effect. Acute Toxicity was assessed using Lethal or Effect Concentrations (LC50/EC50) values. Chronic Toxicity was assessed using Chronic (ChV) values.